

FABRICATION, TREATMENT, AND TESTING OF MATERIALS AND STRUCTURES

The Effect of Composition on the Formation of Light-Emitting Si Nanostructures in SiO_x Layers on Irradiation with Swift Heavy Ions

G. A. Kachurin^a*, S. G. Cherkova^a, D. V. Marin^a, V. G. Kesler^a, V. A. Skuratov^b, and A. G. Cherkov^a

^aInstitute of Semiconductor Physics, Siberian Branch, Russian Academy of Sciences, Novosibirsk, 630090 Russia

*e-mail: kachurin@isp.nsc.ru

^bJoint Institute for Nuclear Research, Dubna, Moscow oblast, 141980 Russia

Submitted August 24, 2010; accepted for publication August 30, 2010

Abstract—The SiO_x layers different in composition ($0 < x < 2$) are irradiated with Xe ions with the energy 167 MeV and the dose 10^{14} cm^{-2} to stimulate the formation of light-emitting Si nanostructures. The irradiation gives rise to a photoluminescence band with the parameters dependent on x . As the Si content is increased, the photoluminescence is first enhanced, with the peak remaining arranged near the wavelength $\lambda \approx 600 \text{ nm}$, and then the peak shifts to $\lambda \approx 800 \text{ nm}$. It is concluded that the emission sources are quantum-confined nanoprecipitates formed by disproportionation of SiO_x in ion tracks due to profound ionization losses. Changes in the photoluminescence spectrum with increasing x are attributed firstly to the increase in the probability of formation of nanoprecipitates and then to the increase in their dimensions; the latter effect is accompanied with a shift of the emission band to longer wavelengths. The subsequent quenching of photoluminescence is interpreted as a result of the removal of quantum confinement in nanoprecipitates and their coagulation.

DOI: 10.1134/S1063782611030122

1. INTRODUCTION

The ability of quantum-confined Si nanocrystals to emit high-intensity radiation in the visible and infrared (IR) regions has attracted the attention of many researchers. The observation of this effect gave hope for the development of light sources for silicon-based optoelectronics. Bulk silicon is unsuitable for such a purpose because of the noncoincidence of the extrema of the conduction band and valence band in position in the Brillouin zone. The properties and the methods of preparation of Si nanocrystals have been currently discussed in a large number of publications. At the present time, Si nanocrystals are commonly formed via self-assemblage upon decomposition of the oversaturated solution of Si in SiO_2 . Such process necessitates heating to temperatures of about 1100°C . At the same time, it was found that Si nanocrystals could be formed also under the influence of short high-power laser pulses [1, 2]. Pulse anneals are rather useful in practice, since such anneals provide a means for locally treating microscopic areas of device systems and for substantially reducing the thermal budget of heating.

Among various types of pulse treatments of materials, irradiation with swift heavy ions (SHIs) occupies a special place. In the beginning of the path inside a target, such ions practically completely spend their energy for ionization. If the stopping rate is higher than $\sim 1 \text{ keV nm}^{-1}$, SHIs penetrating into the target form tracks several nanometers in diameter. Inside the

tracks, the ionization level can be as high as $\sim 10^{22} \text{ cm}^{-3}$ and the temperature can be elevated to 5000 K during 10^{-11} – 10^{-13} s [3]. Thus, SHIs can initiate ionization-stimulated and thermally stimulated processes in solids with a high degree of localization.

Previously, the effect of SHIs on silicon oxides was studied mainly for SiO monoxide layers. In [4], the monoxide layers were irradiated with Ni and Pb ions with the energies 575 and 863 MeV, respectively. The authors of [4] came to the conclusion that, in tracks, the disproportionation of the type $2\text{SiO} \rightarrow \text{Si} + \text{SiO}_2$ took place, with the formation of Si nanocrystals. It was believed that the mechanism of transformation was athermal. The photoluminescence (PL) band with a peak at 600 nm observed after irradiation of the sample was attributed to defects in regions damaged by ions. The authors of [5, 6] studied Si monoxide layers deposited in vacuum onto substrates at 20°C . Irradiation was accomplished with Ni ions (100 MeV) or Ag ions (150 MeV) in the dose range 10^{11} – 10^{14} cm^{-2} . The formation of Si nanocrystals was detected, and emission bands in the violet and yellow-orange regions were observed in the PL spectra. The short-wavelength emission was attributed to defects, whereas the long-wavelength emission to Si nanocrystals. The formation of nanocrystals was thought to proceed by the mechanism of “thermal peaks.” The effect of high-energy Cu ions (50 MeV) on SiO_x layers at $0.1 \leq x < 2$ was studied in [7]. The authors of [7] concluded that, under the influence of ions, SiO_x separated into Si and SiO_2 at all values of x and, in charac-

ter, the separation was spinodal (nucleation-free) decomposition. However, it was impossible to detect Si nanocrystals in the irradiated samples with $0.1 \leq x < 1.5$ by Raman spectroscopy. No data on the luminescence of the nanostructures were reported in [7]. Thus, the properties and the mechanism of formation of light-emitting silicon quantum-confined structures in oxide layers on irradiation with SHIs invite further investigations.

In this study, we try to clarify the question of how an excess Si content influences the formation of light-emitting Si nanostructures in SiO_x layers upon irradiation with SHIs.

2. EXPERIMENTAL

Composition-graded SiO_x layers were deposited onto Si substrates from two atomic fluxes formed by simultaneous magnetron-assisted sputtering of the two sources, fused silica and single-crystal Si, in Ar plasma. The sources were spaced by a distance of about 10 cm. This allowed us to fabricate layers with the composition gradually varying along the substrate length (~ 10 cm) from $\sim \text{SiO}_2$ to $\sim \text{Si}$. The procedure of fabrication of such layers and some of their properties are described in more detail elsewhere [8–10]. The deposited layers were irradiated with Xe ions with the energy 167 MeV and the dose 10^{14} cm^{-2} at room temperature.¹ The path of such ions in both Si and SiO_2 is about 20 μm , the loss for ionization in the deposited layers is 14.5 keV nm^{-1} , and the elastic loss of the Xe ion is 0.3 displacements per nanometer. To study the properties of the layers, we used PL spectroscopy, infrared (IR) transmittance spectroscopy, optical transparency measurements, X-ray photoelectron spectroscopy (XPS), ellipsometry, and high-resolution electron microscopy. To excite the PL signal, we used laser radiation at the wavelength of 488 nm. X-ray photoelectrons were excited with Al $K\alpha$ radiation with the photon energy 1486.6 eV emitted by an Al source. In the XPS measurements, the binding energy was calibrated with reference to the peak of adsorbed carbon with the energy 284.6 eV.

3. RESULTS

The ellipsometry measurements show that the thickness of the formed layer was $\sim 0.55 \mu\text{m}$. The refractive index at the wavelength 632.8 nm gradually varies along the wafer from the “dioxide” end to the “silicon” end in the range from ~ 1.5 to ~ 3.5 (Fig. 1a). The XPS spectra recorded also with displacement of the X-ray beam from the “dioxide” end to the “silicon” end of the wafer show a decrease in the fraction of silicon atoms coordinated with four oxygen atoms

¹ Irradiation was accomplished with the use of the cyclotron ITs-100, Laboratory of Nuclear Reactions, Joint Institute for Nuclear Research.

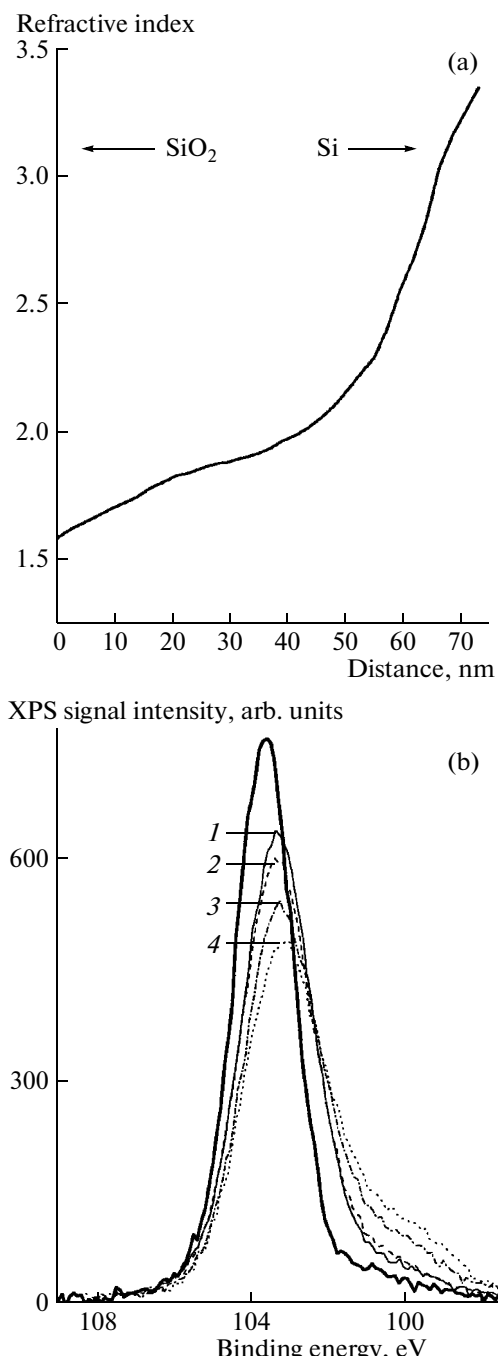


Fig. 1. (a) Variations in the refractive index of the layers along the substrates from the SiO_2 edge to the Si edge. (b) Variations in the XPS spectra along the substrate before irradiation with Xe ions. The distance from the SiO_2 edge is (1) 20, (2) 30, (3) 40, and (4) 50 mm. The thick solid line shows the XPS spectrum of SiO_2 .

and an increase in the number of silicon–silicon bonds (Fig. 1b). The variations in the refractive index along the length of the sample (Fig. 1a), the XPS data for the initial samples (Fig. 1b), the experimentally observed shift of the absorption peak along the sample

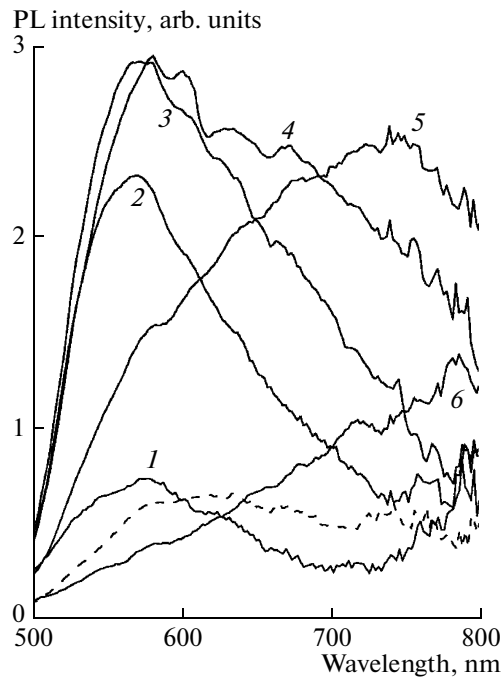


Fig. 2. PL spectra of compositionally different SiO_x layers irradiated with Xe ions. The parameter x is (1) 1.9, (2) 1.85, (3) 1.8, (4) 1.75, (5) 1.7, and (6) 1.65. The dashed line refers to the PL spectrum recorded before irradiation.

in the range $1100\text{--}950\text{ cm}^{-1}$ (not shown), and the results reported in [8–10] allowed us to estimate variations in the Si content in SiO_x . Correspondingly, the substrate was divided into samples with different compositions. Then these samples were irradiated with Xe ions.

The most important results were obtained from studies of the PL spectra before and after ion bombardment of the layers different in Si content. From Fig. 2, it is clear that, in the layers subjected to irradiation, the PL centers responsible for the emission band, whose peak shifts in the wavelength range from ~ 550 to ~ 800 nm, are formed. As the Si content is increased, the PL intensity first increases, with the peak position of ~ 600 nm remaining unchanged. In considering the layers with $x \approx 1.75$ instead of the layers with $x \approx 1.8$, we notice a long-wavelength shoulder appearing in the PL spectrum; even at $x \approx 1.7$, we observe the PL peak shifted to $\lambda \approx 750$ nm. As the excess Si content is increased further, the PL peak shifts to longer wavelengths further and the PL signal is gradually quenched (Fig. 2). Before irradiation with ions, the layers luminesce only slightly and do not exhibit any pronounced dependences of the PL intensity and peak position on the Si content (Fig. 2, dashed line).

To enhance the PL intensity of Si nanocrystals, the nanocrystals are often subjected to low-temperature annealing in hydrogen that passivates the centers of nonradiative recombination of excited charge carriers.

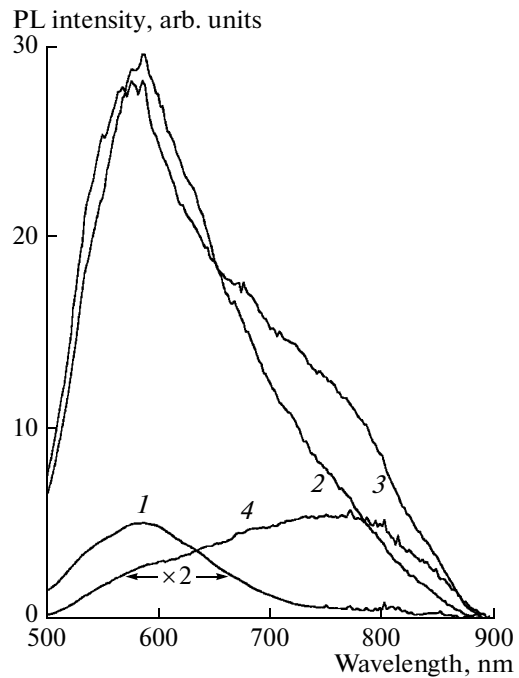


Fig. 3. PL spectra of irradiated SiO_x layers after passivation with hydrogen. The parameter x is (1) 1.95, (2) 1.90, (3) 1.85, (4) 1.65.

We accomplished additional annealing of the samples in the forming gas (94% Ar + 6% H_2) at 500°C for 1 h. The PL spectra of the irradiated samples after being passivated are shown in Fig. 3. For the samples with $x \approx 1.90$ and $x \approx 1.85$, passivation yields a tenfold increase in the PL intensity, with the PL peak position close to 600 nm remaining unchanged. A shift of the PL intensity peak from short wavelength to $\lambda \approx 750\text{--}800$ nm with increasing Si content is observed after passivation as well. A decrease or an increase in the Si content beyond the above-indicated range yields a decrease in the PL intensity and in the efficiency of passivation. It should be noted that passivation slightly enhances also the initially observed low-intensity PL of unirradiated samples, also especially in the short-wavelength region.

In order to identify possible PL sources produced by irradiation with Xe ions, we studied irradiation-induced structural transformation in the layers. It was found that, after irradiation, the transparency of the layers at the wavelength $\lambda = 514.5$ nm was lower (we practically measured the intensity of light transmitted through the sample and reflected back from the substrate). Figure 4 shows the difference between the transparencies of the layers before and after irradiation as a function of x . The higher is Si content in the initial layers, the less transparent the layer after irradiation becomes. This dependence saturates at the Si content corresponding to $x = 1.4\text{--}1.2$, at which the transparency is low initially. Thus, the darkening depends on

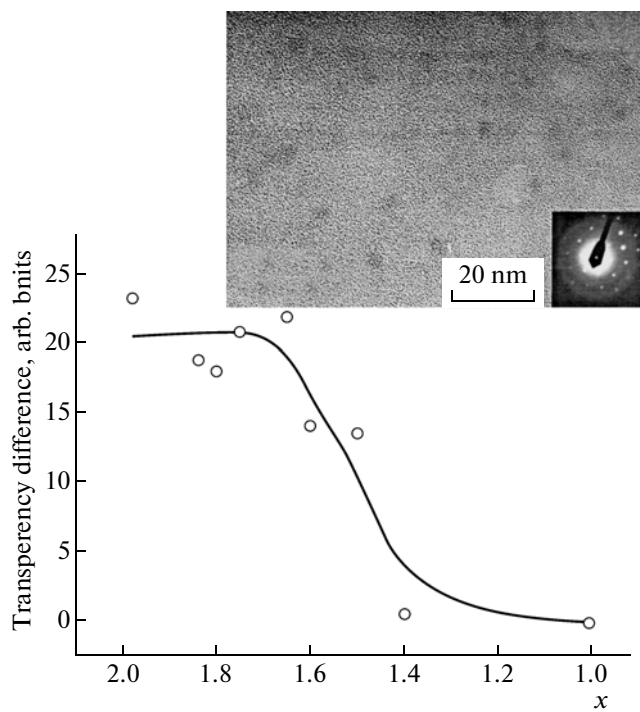


Fig. 4. The difference between the transparencies of the layers before and after irradiation vs. the composition parameter x (see text). Inset: the high-resolution electron microscopy image and the electron diffraction pattern of the SiO_x layer after irradiation with SHI ($x \approx 1.65$).

the Si content; i.e., a decrease in transparency is not associated solely with radiation defects. At the same time, we noticed that annealing in the forming gas at 500°C was favorable to the recovery of the transparency. This effect can be interpreted as a result of partial annealing of defects. By electron microscopy, we detected the formation of dark precipitates ~ 5 nm in dimensions in the irradiated layers (inset in Fig. 4). The diffraction pattern (inset in Fig. 4) involves point reflections corresponding to the Si crystal substrate and a number of highly smeared rings; the spacing between the rings correlates with the position of reflections for the Si crystal. Such rings can be indicative of Si crystal inclusions, but these inclusions are either very small or imperfect.

The inference about the increase in the number of Si–Si bonds on ion bombardment follows from the XPS data. Figures 5a and 5b show the XPS spectra of the Si 2p lines for the SiO_x layers ($x \approx 1.9$) before and after irradiation with Xe ions, respectively. On irradiation, the intensity of the 103.6-eV line of silicon atoms bound with four oxygen atoms is reduced and an extra signal corresponding to lower bonding energies appears. It is known that, with decreasing number of oxygen atoms surrounding a particular silicon atom, the bonding energy of silicon atoms are reduced to 102.4 (1Si–Si–3O), 101.6 (2Si–Si–2O), 100.9

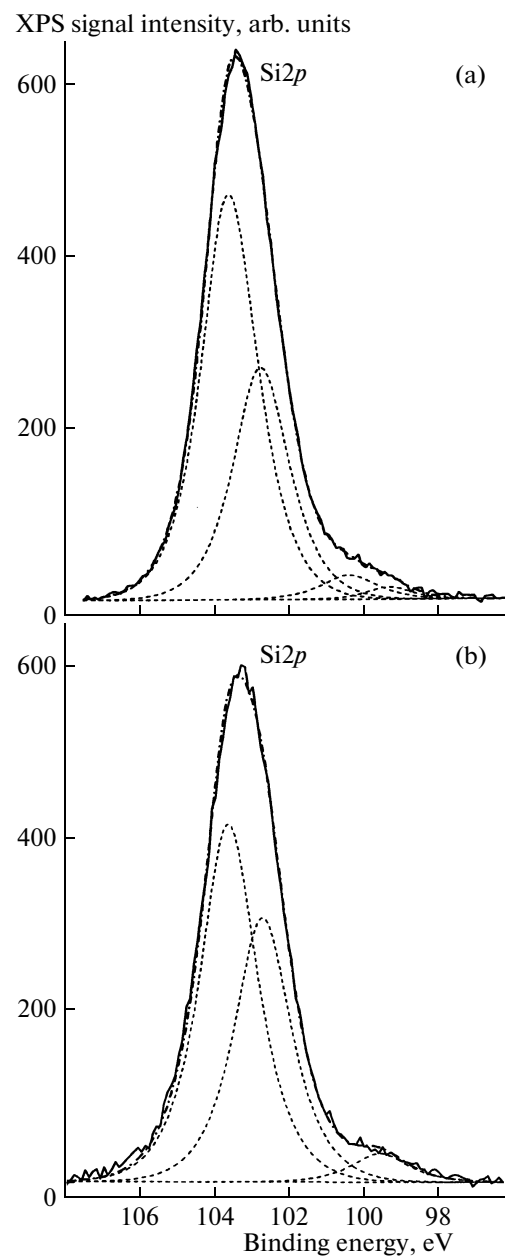


Fig. 5. XPS spectra of the layers (a) before and (b) after irradiation with Xe ions ($x \approx 1.9$). The solid line refers to the experimental spectra. The dashed and dash-dotted lines illustrate, correspondingly, the deconvolution of the spectra by the XPS_Peak program into components and the summation of the component obtained by the deconvolution.

(3Si–Si–1O), and 99.8 eV (Si–4Si). These values of the binding energy were used for automatic deconvolution of the spectra with the use of the program XPS_Peak. From Fig. 5, it is evident that the fraction of Si atoms bound to four O atoms is decreased and the fraction of Si atoms bound to four Si atoms is increased by a factor of about four. The intensity of the 102.4-eV line is also increased. In the samples with the higher initial Si content, we observe a shift of the Si

$2p$ line of the Si phase (99.8 eV) to lower binding energies. Such a shift can occur due to formation of charged conducting clusters in an insulator medium. It should be also noted that irradiation with Xe ions induces a decrease in the Auger parameter for all of the samples. This effect can be caused by the formation of partially crystallized structures.

4. DISCUSSION

The data presented above show that irradiation-induced changes in the PL spectra of the layers depend on the Si content and are accompanied by structural transformations. As the Si content is increased, an increase in the intensity of the PL signal with a peak at $\lambda \approx 550\text{--}600$ nm prevails first, and then we observe a shift of the peak to $\lambda \approx 750\text{--}800$ nm (Fig. 2). Observation of such behavior gives us grounds to believe that the enhancement of the PL signal is due to the increase in the number and dimensions of emission sources that experience quantum confinement. In some studies, the yellow-orange emission was attributed to defects in the oxide; however, from our point of view, the key role is played by differently sized and shaped Si nanoprecipitates [11–14]. We believe that, in the case under consideration, the sources of the PL signal are quantum-confined nanoinclusions formed under the influence of FHIs. The increase in the number of nanoprecipitates yields an increase in the PL intensity, and the increase in the precipitate dimensions yields a shift of the PL band to longer wavelengths. The large excess of silicon involves the growth of precipitates, with the removal of quantum-confinement conditions, and the coalescence of precipitates. Both of these factors quench the PL signal.

This interpretation is supported by observation of a number of effects of FHIs on the layers. These effects are as follows: a decrease in the transparency dependent on the excess of Si in the samples (Fig. 4), the formation of nanoprecipitates observed with an electron microscope (Fig. 4), an increase in the number of Si–Si bonds (Fig. 5), and the shift of the PL signal to longer wavelengths with increasing Si content in the layers (Fig. 2). The above inference is confirmed also by the characteristic response of the layers to passivating anneals, specifically, by the substantial enhancement of the PL signal (Fig. 3). If the PL signal were due to defects, we would have more reasons to expect a decrease, rather than an increase, in the PL intensity upon passivation of the samples with hydrogen.

Profound changes in the PL spectra were observed in a rather narrow region of decreasing x (increasing Si content). At $x \approx 1.85$, the decrease in x is accompanied by an increase in the PL intensity with no visible shift of the peak from 600 nm; however, even at $x \approx 1.80$, the appearance of a long-wavelength shoulder can be

noted, and at $x \approx 1.7$, the PL peak is found to be shifted to $\lambda \approx 750$ nm (Fig. 2). Such behavior of the PL signal can be explained as described below. There exist two structural models of the SiO_x layers, specifically, the random bonding model and the composite medium model. In the former model, it is assumed that the Si and O atoms and the Si–O bonds are arranged randomly. In the other model, it is assumed that the structure presents a mixture of different separated phases. The PL data obtained for the initial layers (Fig. 2), the response of the layers to passivating anneals, and especially the XPS results (Fig. 1) suggest that, even before irradiation, the layers involve regions enriched to some degree with silicon. Therefore, we may assume that, most likely, the SiO_x layers studied here correspond to the composite medium model. In general, such composite state is typical of the layers produced by plasma methods [15], whereas the structure of the layers produced by vacuum evaporation is closer to the random bonding model [16]. We believe that, at a small excess of Si, only a limited number of Si-enriched regions capable of being transformed into short-wavelength PL centers under the influence of SHIs fall into the ion tracks. As the Si content is increased, at first, mainly the probability that the regions with the minimal Si content required for the formation of centers of emission at $\lambda \approx 600$ nm fall into the tracks increases. Therefore, with decreasing x , at first, mainly the number of emission centers grows and, correspondingly, the PL intensity at about 600 nm increases. As the Si content is increased further, the Si-enriched regions become larger in size, denser, and closer to each other. Due to all these factors, the final size of nanoprecipitates becomes rather large, resulting in the shift of the PL peak to $\lambda \approx 750$ nm because of the size-quantization effect. The decrease in the PL intensity at a very high excess Si content is due to the breakage of quantum confinement and the coagulation of precipitates.

It is still hard to tell whether the formation of nanoprecipitates is a thermal process or an athermal (ionization) process. Diffusive drain to nuclei in the solid oxide can be ruled out, since the diffusion coefficients of silicon atoms, as well as oxygen atoms, are too small. In the composite medium model, the problem of how Si atoms gather to form nanoprecipitates is simplified, especially if it is assumed that the material inside tracks goes through the stage of melting. Electrons in the track are thermalized in $\sim 10^{-15}$ s, whereas for the energy transfer to atoms, the time of $\sim 10^{-11}$ s is needed. Then the track is cooled with the rate up to $\sim 10^{13}$ K s⁻¹. In the stage of melting, the material can be for $10^{-10}\text{--}10^{-9}$ s. At the diffusion coefficients in melts $10^{-3}\text{--}10^{-4}$ cm² s⁻¹, the time of $10^{-10}\text{--}10^{-9}$ s is long enough for Si atoms to form nanoclusters. Moreover, it was shown by the molecular dynamic method that decomposition of the oxide into Si and SiO_2 took place

even in the SiO_x melt and the precipitates were larger in size at a higher Si content [17]. The conditions for nucleation in SHI tracks were treated theoretically in [18]. Thus, the formation of nanoclusters can be understood in the context of the thermal mechanism. At the same time, in some studies concerned with femtosecond pulse laser annealing, it was noted that structural transformations in the irradiated layers started to proceed even before the excited electrons had managed to transfer an energy large enough to melt the material [19–21].

It should be finally noted that the maximum PL intensity of the irradiated samples is attained at $x \approx 1.8$, whereas in the case of common annealing, the optimum of the PL intensity is observed at much larger excess of Si, ~10–20 at % ($x = 1.5\text{--}1.1$) [8, 15, 22, 23]. It seems likely that, due to high ionization levels and temperatures, more Si–O bonds dissociate in tracks [24, 25].

5. CONCLUSIONS

It is found that irradiation of SiO_x layers with Xe ions with an energy of 167 MeV brings about the formation of visible PL sources, the properties of which systematically vary under variations in the composition of the layers. As the Si content in the layers is increased, the PL band intensity with a peak at about 600 nm first increases and then shifts to the longer wavelengths 750–800 nm. Changes in the PL spectra with increasing Si content in the layers are attributed to the increase in the number of emission sources and in their dimensions that define the quantum-confinement conditions for excited charge carriers. From the data of electron microscopy, XPS spectrometry, and optical transparency measurements, as well as from the response of the PL signal to passivation of the samples with hydrogen, it is concluded that the role of emission sources is played by silicon nanoprecipitates formed on disproportionation of SiO_x in SHI tracks. Formation of the nanostructures is possible due to intense short-time heating of the material inside the tracks. An increase in the excess Si content in the initial layers yields, first, an increase in the probability of formation of nanoprecipitates and, thus, an increase in the PL intensity and, then, an increase in the dimensions of nanoprecipitates. The last-mentioned effect results in a shift of the PL band to longer wavelengths due to quantum confinement. The decrease in the PL intensity at a very high excess Si content is due to the break of quantum-confinement conditions and the coagulation of nanoprecipitates.

ACKNOWLEDGMENTS

We thank Z.Sh. Yanovitskaya for placing the samples at our disposal, V.A. Volodin for his help in con-

ducting optical measurements, and V.V. Kirienko for conducting annealing of the samples in the forming gas.

This study was supported in part by the Russian Foundation for Basic Research, project no. 08-02-00221a.

REFERENCES

1. G. A. Kachurin, I. E. Tyschenko, K. S. Zhuravlev, N. A. Pazdnikov, V. A. Volodin, A. K. Gutakovskiy, A. F. Leier, W. Skorupa, and R. A. Yankov, Nucl. Instrum. Methods Phys. Res. B **112**, 571 (1997).
2. G. A. Kachurin, S. G. Cherkova, D. V. Martin, R. A. Yankov, and M. Deutschmann, Nanotechnology **19**, 355305 (2008).
3. M. Toulemonde, Ch. Dufour, A. Meftah, and E. Paumier, Nucl. Instrum. Methods Phys. Res. B **166**–**167**, 903 (2000).
4. D. Rodichev, Ph. Lavallard, E. Dooryhee, A. Slaoui, J. Perriere, M. Gandais, and Y. Wang, Nucl. Instrum. Methods Phys. Res. B **107**, 259 (1996).
5. P. S. Chaudhari, T. M. Bhave, D. Kanjilal, and S. V. Bhoraskar, J. Appl. Phys. **93**, 3486 (2003).
6. P. S. Chaudhari, T. M. Bhave, R. Pasricha, F. Singh, D. Kanjilal, and S. V. Bhoraskar, Nucl. Instrum. Methods Phys. Res. B **239**, 186 (2005).
7. W. M. Arnolddik, N. Tomozeiu, E. D. van Hattum, R. W. Lof, A. M. Vredenberg, and F. H. P. M. Habraken, Phys. Rev. B **71**, 125329 (2005).
8. M. Dovrat, Y. Goshen, J. Jedrzejewski, I. Balberg, and A. Sa'ar, Phys. Rev. B **69**, 155311 (2004).
9. A. N. Karпов, D. V. Marin, V. A. Volodin, J. Jedrzejewski, G. A. Kachurin, E. Savir, N. L. Shvarts, Z. Sh. Yanovitskaya, Y. Goldstein, and I. Balberg, Fiz. Tekh. Poluprovodn. **42**, 747 (2008) [Semiconductors **42**, 731 (2008)].
10. S. N. Shamin, V. R. Galakhov, V. I. Aksenova, A. N. Karпов, N. L. Shvarts, Z. Sh. Yanovitskaya, V. A. Volodin, I. V. Antonova, T. B. Ezhevskaya, J. Jedrzejewski, E. Savir, and I. Balberg, Fiz. Tekh. Poluprovodn. **44**, 550 (2010) [Semiconductors **44**, 531 (2010)].
11. P. Mutti, G. Ghislotti, S. Bertoni, L. Bonoldi, G. F. Cerofolini, L. Meda, E. Grilli, and M. Guzzi, Appl. Phys. Lett. **66**, 851 (1995).
12. G. Ghislotti, B. Nielsen, P. Asoka-Kumar, K. G. Lynn, A. Gambhir, L. F. DiMauro, and C. E. Bottani, J. Appl. Phys. **79**, 8660 (1996).
13. S. P. Withrow, C. W. White, A. Meldrum, J. D. Budai, D. M. Hembree, Jr., and J. C. Barbour, J. Appl. Phys. **86**, 396 (1999).
14. Y. Batra, T. Mohanty, and D. Kanjilal, Nucl. Instrum. Methods Phys. Res. B **266**, 3107 (2008).
15. T. G. Kim, C. N. Whang, Y. Sun, S.-Y. Seo, J. H. Shin, and J. H. Song, J. Appl. Phys. **91**, 3236 (2002).
16. H. Rinnert, M. Vergnat, and A. Burneau, J. Appl. Phys. **89**, 237 (2001).
17. S. Q. Wu, C. Z. Wang, Z. Z. Zhu, and K. M. Ho, Appl. Phys. Lett. **96**, 043121 (2010).

18. A. Volkov, Nucl. Instrum. Methods Phys. Res. B **193**, 376 (2002).
19. T. Y. Choi, D. J. Hwang, and C. P. Grigoropoulos, Opt. Eng. **42**, 3383 (2003).
20. K. Sokolowski-Tinten, J. Bialkowski, and D. von der Linde, Phys. Rev. B **51**, 14186 (1995).
21. H. W. K. Tom, G. D. Aumiller, and C. H. Brito-Cruz, Phys. Rev. Lett. **60**, 1438 (1998).
22. M. Lopez, B. Garrido, C. Bonafos, A. Perez-Rodrigues, J. R. Morante, and A. Claverie, Nucl. Instrum. Methods Phys. Res. B **178**, 89 (2001).
23. G. A. Kachurin, S. G. Cherkova, V. A. Skuratov, D. V. Marin, and A. G. Cherkov, Fiz. Tekh. Poluprovodn. **44**, 544 (2010) [Semiconductors **44**, 525 (2010)].
24. G. S. Chen, C. B. Boothroyd, and C. J. Humphreys, Appl. Phys. Lett. **62**, 1949 (1993).
25. M. Takeguchi, K. Furuya, and K. Yoshihara, Jpn. J. Appl. Phys. **38**, 7140 (1999).

Translated by E. Smorgonskaya